FRACTURE MECHANICS ANALYSES OF THE SHEAR FAILURE IN A CONCRETE BRIDGE

Mario Plos, M.Sc., Research Assistant

Kent Gylltoft, Ph.D., pro tem. Professor

Division of Concrete Structures
Chalmers University of Technology, Sweden

ABSTRACT

The shear behaviour of a portal frame concrete bridge, previously loaded to failure in a full scale test, was analysed using the non-linear finite element method. The constitutive models for concrete were based on fracture mechanics and both the smeared and discrete crack approaches were used. The analysis based on the discrete crack approach was successfully performed up to a stage where final failure was initiated. The analysis based on the smeared crack approach, however, could be performed until final failure, only if large residuals were allowed. The analysis based on the discrete crack approach was found to be laborious. The smeared crack approach is indeed more general and significant progress will be achieved when the numerical difficulties connected with this approach are reduced.

The use of fracture mechanics in combination with the non-linear finite element method is considered to be a most powerful tool for obtaining a better understanding of the failure process. More research is proposed, however, to make it possible to use the method in a rational manner in the search for design methods that are based on the real mechanics of failure.

Key words: Reinforced concrete, Fracture mechanics, Non-linear finite element analysis, Concrete bridges, Shear failure.

1 INTRODUCTION

1.1 Background

Fracture mechanics has been used to form constitutive models for concrete in several non-linear finite element programs. With these material models, concrete structures can be modelled more accurately, taking the progressive cracking under increased load into account. Such an analysis corresponds more accurately to the real physical behaviour of a structure than conventional design models.

Full scale tests have been carried out to evaluate the shear capacity of two highway concrete bridges north of Göteborg, Sweden, in 1989, see Plos *et al.* /1-3/. The test results revealed shortcomings in the conventional design models in the Swedish Concrete Codes, BBK 79 /4/. It was found that further research was needed to develop models that describe more closely the actual behaviour when a structure is loaded to failure. Accordingly, finite element analyses based on fracture mechanics were made for one of the bridges tested, a portal frame bridge, in order to improve knowledge of the real response of a large structure loaded to shear failure.

1.2 Aim and Scope

The objective of this study was to analyse the behaviour of a large and complex structure using the non-linear finite element method and material models based on fracture mechanics. The highway bridge tested was analysed, therefore, to study its behaviour when loaded to failure. Another aim was to examine how well such an analysis can be performed with available finite element programs and how laborious such an analysis is. Both discrete and smeared crack approaches were used and various numerical solution methods were tested. The results of the analysis were compared with the cracking observed during the test, as well as with the measured loads, deflections and strains.

The finite element program ABAQUS, see HKS /5/, was used for the analyses. For the smeared crack analysis, the concrete material model available within ABAQUS was used. For the analysis based on the discrete crack approach, the non-linearity caused by cracking of the concrete was modelled by non-linear springs between elastic solid elements. The reinforcement was modelled using an option, called rebar in ABAQUS, that strengthens the concrete elements in a specified direction. The bridge models were two-dimensional and the analyses were performed with the assumption of plane stress state. Only the bridge deck slab was modelled in detail. The behaviour of the support and wing walls, together with the supporting earth around the walls, was modelled by non-linear springs at the ends of the bridge deck slab. The complete load history of the bridge was modelled, including traffic load before the test, addition of the steel plates to the bridge and the final loading to failure.

2 THE BRIDGE AND THE FULL SCALE TEST

The bridge analysed was a conventionally reinforced portal frame bridge with a free span of 21 m, see Figure 1. It consisted of a slab that was joined to wall supports and wing walls, forming a frame. In the original design of the bridge, the reinforcement of the slab was shortened and anchored in accordance with the variation of the bending moment caused by traffic loads. In the test, however, the bridge was loaded so that the moment distribution was different from that of the original design. To obtain a shear failure, it was necessary to increase the moment capacity of the bridge by gluing longitudinal steel plates to the underside of the bridge deck, see Täljsten /6/. The underside of the bridge deck slab was cracked already, before the test, in an area of about six meters, centred around the middle of the bridge span.

The bridge was loaded 4.00 m from one of the supporting walls to induce shear failure. The load was applied using tension rods anchored in the rock foundation under the bridge. The bridge

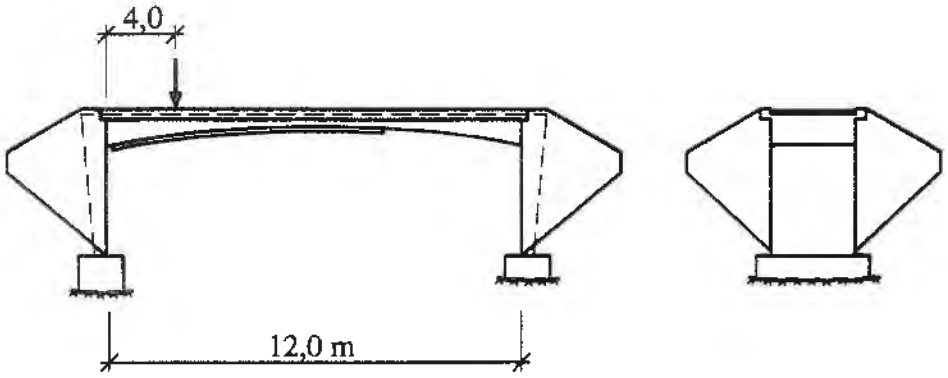

Fig. 1. Portal frame concrete bridge, loaded to failure in a full scale test and analysed with the nonlinear finite element method.

failure can be regarded as a typical shear failure, see Figure 2. Just prior to failure, the bridge deck was extensively cracked at the bottom of the slab, mostly with vertical cracks, and some vertical cracks had occurred at the top of the deck close to the supports, see also Figure 15b. As can be seen in Figure 2, the failure was caused by a crack that had a smaller angle to the horizontal axis than the few previous inclined cracks. It occurred suddenly in a part of the deck that was previously uncracked. One reason why this crack determined the failure was that the crack path did not cross any of the glued steel plates, i.e. the steel plates did not contribute to holding this crack together, nor did they transfer forces across the crack.

3 FRACTURE MECHANICS MODELS

3.1 General

When concrete starts to crack, microcracking is localized in a crack band zone, in which a main crack finally forms. A constitutive relationship can therefore be expressed as a combination of

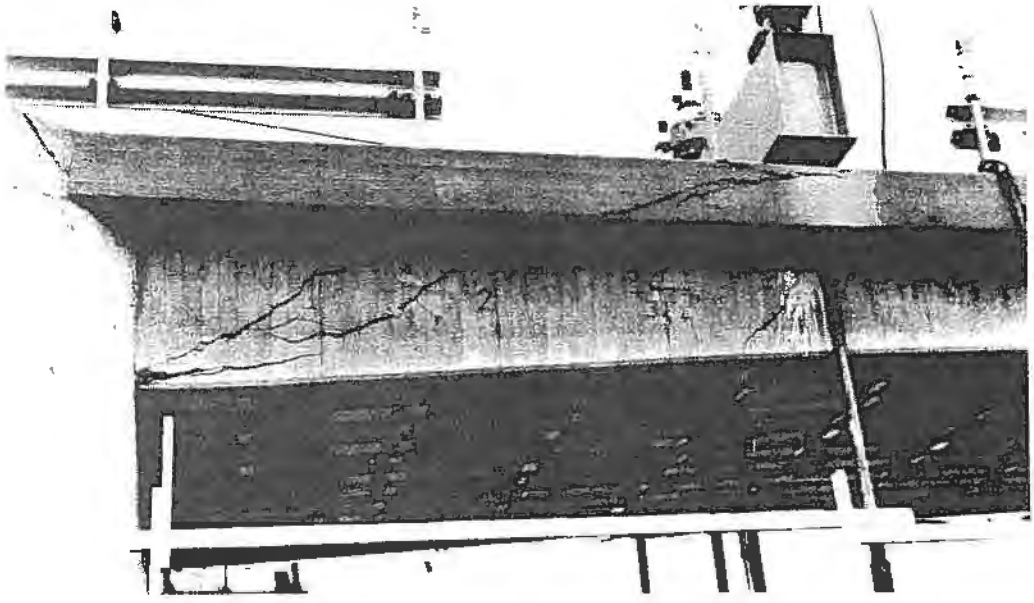

Fig. 2. Shear failure of the bridge

elastic response for the material continuum and an additional stress-deformation relation for the crack band zone see Elfgren *et al.* /7/.

In the smeared crack approach, the non-linearity of the crack band zone is expressed by an elastic-plastic material model. The localized material non-linearity is smeared out and the material response in tension is expressed as a stress-strain relationship for the material including cracks.

In the discrete crack approach, the non-linearity of the microcracking is approximated as being localized to a discrete crack with no width before cracking starts. The material response in tension is expressed as a stress-displacement relationship, describing the opening of the crack, in combination with elastic material response for the material between the cracks.

The material properties for concrete, used in the analyses, were based on the measured compressive and splitting tensile strength. The measured compressive strength was recalculated to a corresponding wet cylinder strength, f_{cc} = 42 MPa, which was used in the analysis. The modulus of elasticity was approximated to E_c = 42 GPa according to the Concrete Handbook Material, see AB Svensk Byggtjänst and Cementa AB /8/. Poisson's ratio was approximated to be $\nu = 0.2$. The fracture energy was approximated to 130 N/m according to test data presented by Pettersson /9/ and Hordijk *et al.* /10/.

3.2 The Smeared Crack Model

The material model used to model the concrete in the smeared crack analysis was the concrete model available in ABAQUS, see HKS /5/. The concrete model can be described schematically as an elastic-plastic material model, based on the smeared crack approach. The elastic stress state is limited by a Drucker-Prager yield surface when the stress state is dominantly compressive, and by a "crack detection surface" in tension, see Figure 3. In compression, yielding is modelled using associated flow with isotropic hardening. When cracking occurs in tension, the crack orientation is stored and damage elasticity is used to model the material behaviour in the direction perpendicular to the crack. The stress components associated with an opening crack are not included in

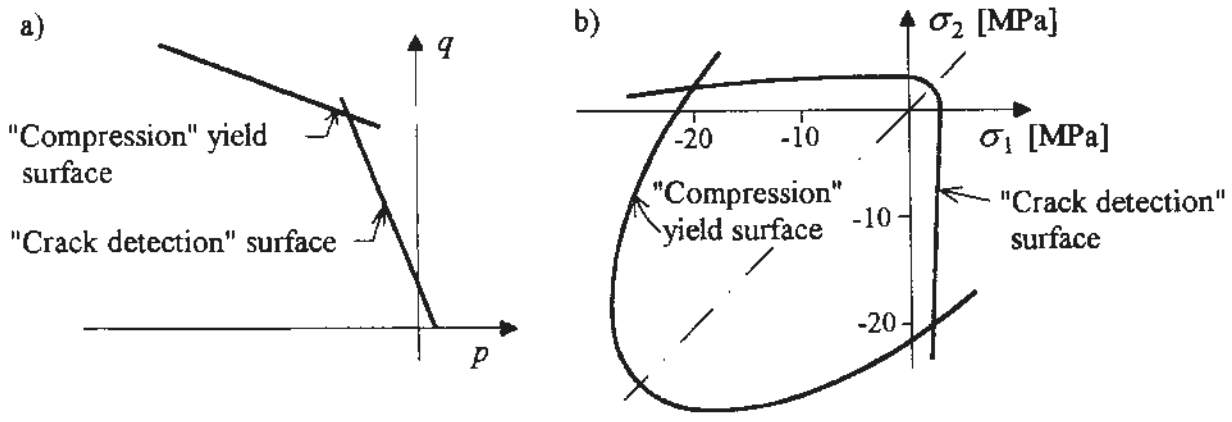

Fig. 3. Concrete failure surfaces (a) in the p-q-plane (where p is hydrostatic stress and q is deviatoric stress), and (b) in the σ_1-σ_2-plane (plane stress: $\sigma_3 = 0$). The relations are shown for a stress state before yield in compression or cracking is initiated.

the definition of the crack detection surface. Additional cracks will form only in directions orthogonal to the existing crack.

When concrete is unloaded in compression, the material model provides for unloading by using the initial elastic stiffness. In tension, damage elasticity is used, and unloading is done using a lower modulus of elasticity so that no permanent strain remains across a crack. Accordingly, cracks will close completely if the stress across the crack becomes zero, see Figure 4.

The shape of the uniaxial stress-strain relationship in compression was chosen to match typical test data presented by Kupfer and Gerstle /11/, see Figure 4. In tension, the stress-displacement relation for the crack band was recalculated to a stress-strain relation. The strain values were calculated by dividing the crack band opening by the mean crack distance, in order to represent the actual overall behaviour of the bridge correctly. Consequently the mean distance between bending cracks had to be predicted and was approximated here as the mean distance between visible cracks registered during the test, $s = 0.25$ m. The tensile strength was finally approximated to be $f_{ct} = 2.5$ MPa. The descending branch of the stress-strain relation in tension was approximated according to Figure 4, and the shape of the curve was smoothed to minimize numerical problems due to sudden changes of the structural stiffness in the finite element analysis.

ABAQUS offers the opportunity to define a "shear retention factor" that is used to reduce the shear modulus in the crack plane. In the preliminary analyses, no significant difference could be observed between different reductions of this factor. In the final analysis, the shear modulus was directly reduced to zero when cracking started.

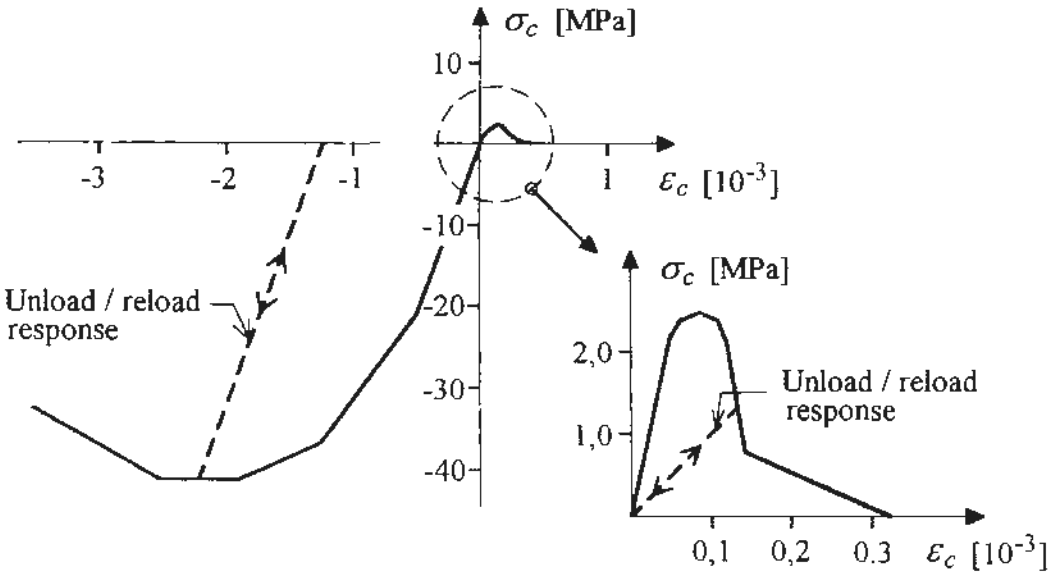

Fig. 4. The uniaxial stress-strain relationship, used in the smeared crack analysis. In tension, the curve was smoothed to minimize numerical problems, while the total fracture energy was kept constant.

3.2 The Discrete Crack Model

For the discrete crack analysis, non-linear spring elements were used to model the cracks, while the material between the cracks was modelled by linear elastic elements. The spring elements were oriented both perpendicular and parallel to the cracks, providing force-displacement relations between the nodes on either side of the crack. The force-displacement relations were calculated from the stress-displacement relation for the crack band. The forces were calculated by integrating the stresses along the crack, between the mid-points between the node of interest and the nodes closest to it. The displacements in the spring properties were adjusted with regard to differences between the crack distance in the model and the mean crack distance, measured in the test.

The spring elements were given zero length at the start of the calculation. However, since the spring elements within ABAQUS require an elastic part of the force-displacement relation, a small dummy length of one millimetre was introduced in calculating the elastic stiffness. The same elastic stiffness was used in compression. The tensile strength was approximated to be $f_{ct} = 2.5$ MPa for the bending cracks in the discrete crack analysis.

In the analysis, the model had to be unloaded after it had been subjected to "traffic load". Unloading of the cracks, however, could not be modelled using non-linear springs. Instead, the analysis was ended and a new analysis started with modified material behaviour in tension, where cracking had occurred. Figure 5 shows how the force-displacement relation was changed for a spring where cracking had started before unloading.

The shear properties parallel to the cracks were modelled with springs parallel to the cracks. The shear springs were given elastic, perfectly plastic properties. The elastic properties corresponded to the elastic shear stiffness of the concrete across a crack band width of one millimetre, and the yield strength was approximated to be equal to the tensile strength of the concrete. Linear elastic

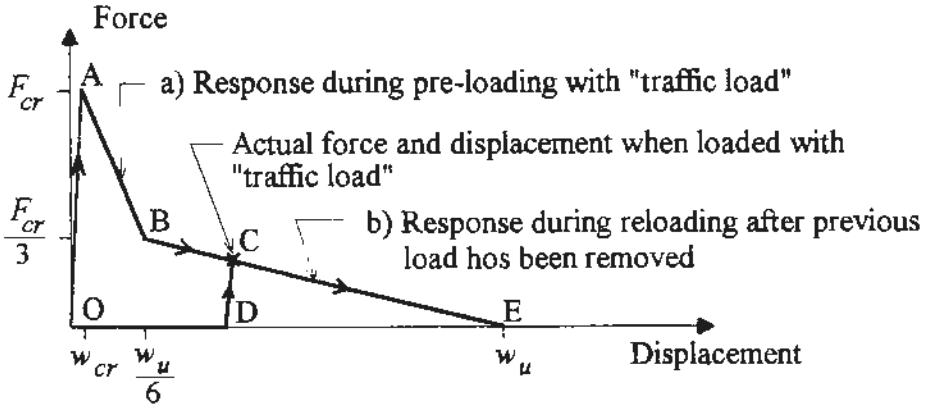

Fig. 5. Example of a force-displacement relation for a concrete spring perpendicular to a crack. For "traffic load", the spring response follows curve a) from O over A and B to point C. To enable the modelling of the crack behaviour when the bridge was reloaded after the "traffic load" had been removed, the force-displacement relation was redefined. The partly cracked concrete was modelled by curve b), going from O over D, C and E, which was used in the analysis of the test.

material was assumed between the cracks. The compression stresses were ascertained, from the output of the analysis, to be within the elastic part of the concrete response.

3.3 Constitutive Models for the Reinforcement and the Steel Plates

The constitutive behaviour of the steel in the reinforcement and in the steel plates was modelled by a linear elastic, perfectly plastic material model. The modulus of elasticity was approximated to be E_s = 200 GPa, and Poisson's ratio to be ν = 0.3. The main reinforcement was of the quality Ks 600, and the yield strength was approximated to f_{sy} = 600 MPa. The steel plates had a yield strength of f_{sp} = 640 MPa.

In the smeared crack analysis, the effect of the reinforcement was superimposed on the concrete elements by the rebar option provided in ABAQUS. The specified rebars strengthened the concrete elements in the direction of the reinforcement.

In the discrete crack analysis, the effect of the reinforcement in the bending cracks was modelled by superimposing the force-displacement relation of the reinforcement on the corresponding concrete relation perpendicular to the crack. In the shear crack, additional reinforcement springs, acting in the reinforcement direction, were added to the concrete springs.

Before the cracking of the concrete, elastic material and complete interaction between reinforcement and concrete were assumed. After cracking of the concrete, the force-displacement relation for the reinforcement was modelled considering that the reinforcement force in the crack was gradually transferred to the concrete by the bond between the reinforcement and the surrounding concrete, see Figure 6.

The force-displacement relation was approximated by a linear relation up to the yielding point of the reinforcement. In order to determine the crack width associated with the yield force, the shear stress along the reinforcement was approximated to decrease linearly from a maximum stress, $f_{cs} = f_{cp}$ close to the crack, to zero where the whole yield force was transferred to the surrounding concrete, see Figure 7. Where the mean crack distance was too short for the whole yielding force to be transferred to the concrete, the same decrease of shear stress was assumed. As in the

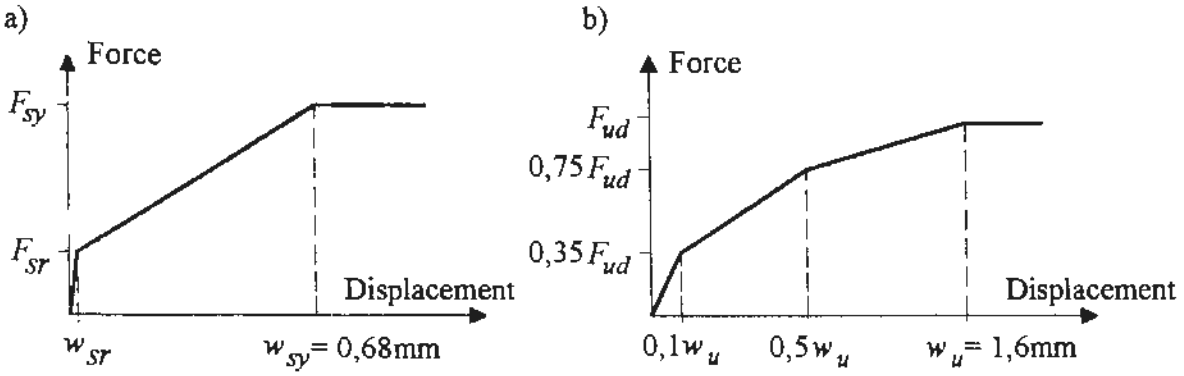

Fig. 6. Force-displacement relation a) for reinforcement springs over a crack in the longitudinal direction of the reinforcement, and b) for springs modelling the dowel action, acting perpendicular to the reinforcement.

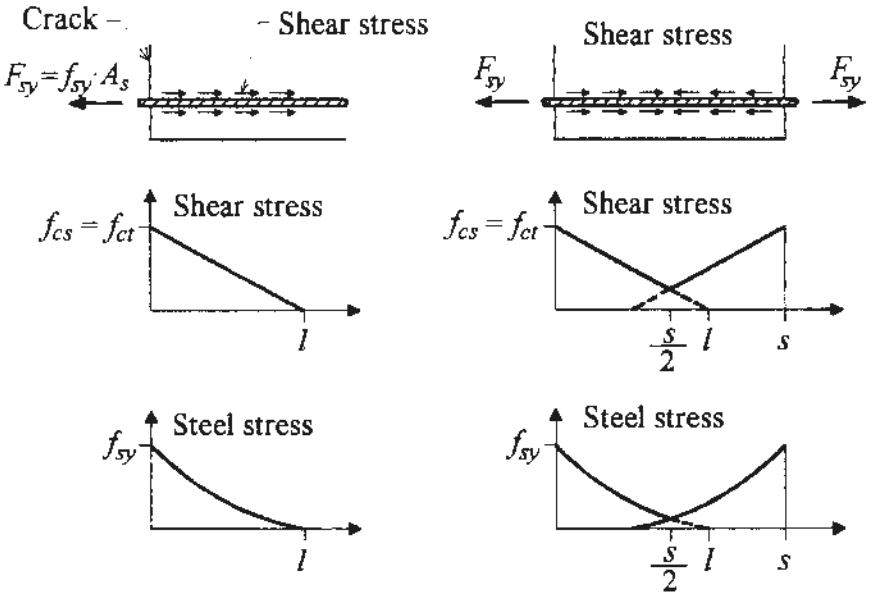

Fig. 7. A simplified assumption regarding the bond stress along the reinforcement is used for determining the crack width when the steel yields, w_{sy}. If the distance between the cracks is longer than twice the transfer length, l, see a), then w_{sy} is calculated as twice the reinforcement elongation along the transfer length. If the distance between the cracks is shorter than $2 \cdot l$, see b), then w_{sy} is calculated as twice the reinforcement elongation along half the crack distance.

smeared crack analysis, the mean crack distance was approximated to be $s = 0.25$ m.

The dowel action of the reinforcement was considered in the shear crack by springs perpendicular to the reinforcement direction. The shape of the force-displacement was approximated from test results on studs, presented by Johnsson and Molenstra /12/ and Ollgaard *et al.* /13/, while the maximum force and displacement values were calculated according to the CEB-FIP Model Code, see CEB /14/.

The steel plates were modelled by truss elements and, in the discrete crack analysis, by springs over the cracks in the directions of the plates. The force-displacement relation for the springs was determined in the same way as for the reinforcement, and the crack width at steel yielding was approximated to be $w_{sy} = 1.5$ mm.

4 FINITE ELEMENT ANALYSES OF THE BRIDGE

4.1 The Finite Element Model with the Smeared Crack Approach

The finite element model based on the smeared crack approach was two-dimensional and consisted mainly of plane stress elements. Eight-node quadrilateral elements, complemented with six-node triangular elements, were used to model the bridge deck slab, see Figure 8. The concrete material model available in ABAQUS was used in combination with the rebar option for the reinforcement. Each layer of reinforcement was defined separately, strengthening the element it belonged to in the longitudinal direction of the reinforcement. The steel plates were modelled by

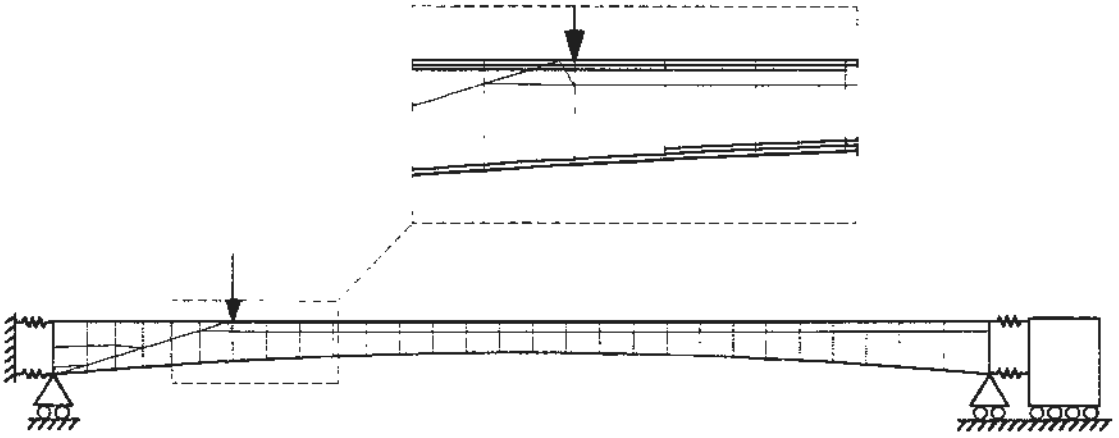

Fig. 8. Element mesh and boundary conditions for the smeared crack model. The positions of the superimposed reinforcement layers are shown in the magnified part.

three-node truss elements.

The boundary conditions for the bridge deck were modelled using simple supports and a pair of non-linear springs at each end of the slab. The end cross sections of the bridge deck slab were forced to remain planar throughout the analysis. The non-linear springs were used to model the behaviour of connecting parts of the structure, as well as the influence of soil around the structure. The properties of the springs were determined by a simpler finite element analysis, where the bridge deck consisted of non-linear beam elements. The stiffness changes of the beam elements were calculated from the registered crack development in the bridge during the test, and the load-deflection relations of the springs were adapted, so that the deflections of the model matched the measured deflections of the test.

4.2 The Finite Element Model with the Discrete Crack Approach

The finite element model based on the discrete crack approach consisted mainly of elastic, plane stress elements and non-linear spring elements to model the crack behaviour. To model the concrete between the cracks, four-node quadrilateral and three-node triangular elements were used, see Figure 9. To model the cracks, spring elements were used in pre-defined crack sections. The steel plates were modelled by two-node truss elements, attached to the bottom of the elastic bridge deck elements, and by spring elements over the crack sections. Figure 10 is a detail of the left end of the bridge model, showing the elements included in the analysis.

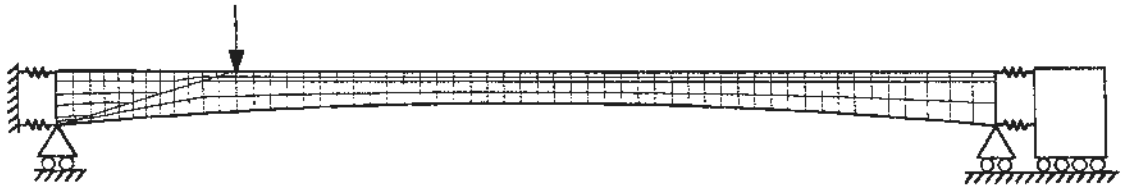

Fig. 9. Element mesh and boundary conditions for the discrete crack model.

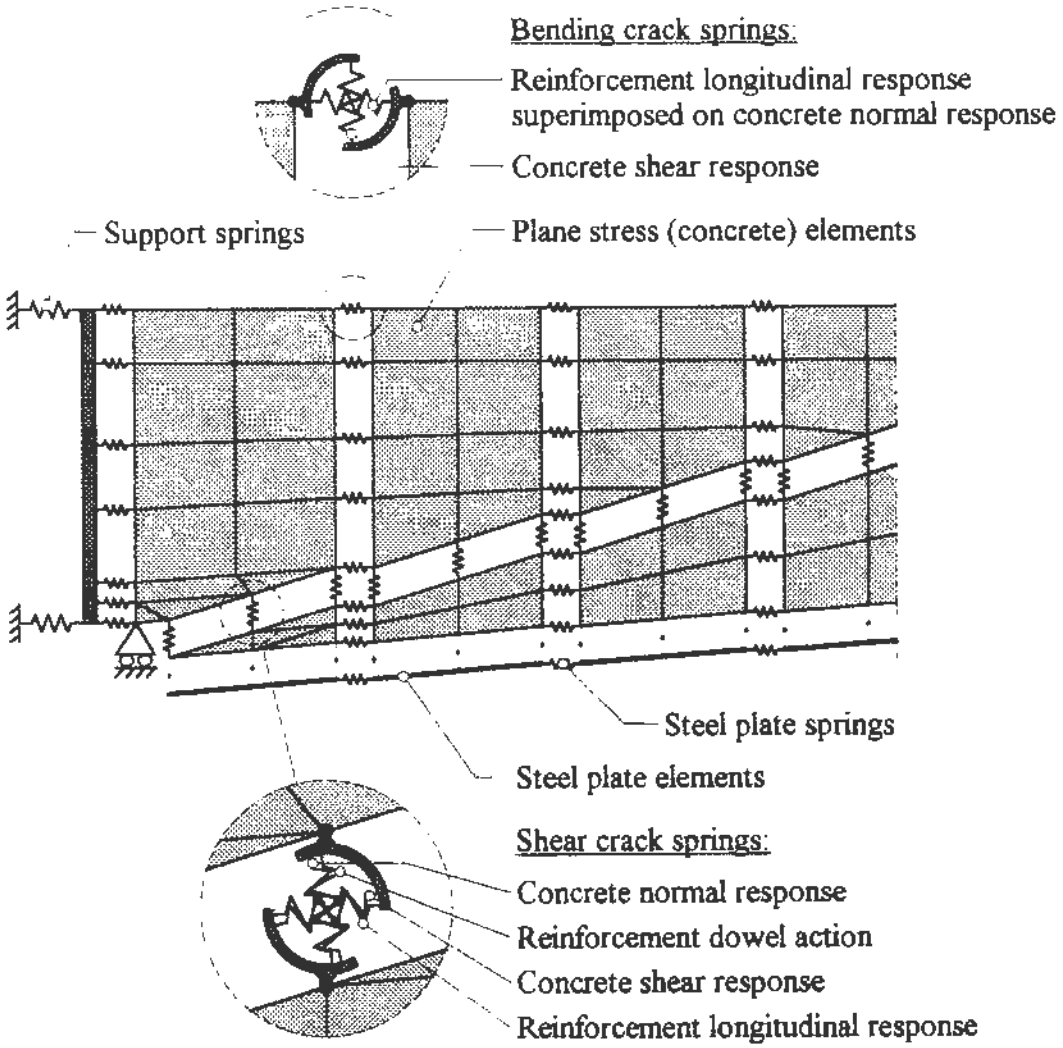

Fig. 10. Detail showing, for the discrete crack model, the end with the shear crack. The solid elements at both sides of the cracks are moved apart, here, and the springs across the cracks are shown schematically. In the bending cracks, the reinforcement response was superimposed on the concrete response in the springs perpendicular to the cracks. In the shear crack, additional springs were added to model the reinforcement behaviour.

The orientation of the crack sections was determined from the crack distribution observed in the test. In order to reduce the size of the model, and to minimize numerical problems in the analysis the spacings between the crack sections were made larger than in the test. The load-deformation relations for the springs were corrected for this, as mentioned in Section 3.2. The boundary conditions were modelled in the same way as in the model based on smeared crack approach.

4.3 Solution Methods

The load history of the bridge was accounted for by performing the finite element analyses in several subsequent load steps. In each load step a load, a prescribed deformation, or a combination of several loads or prescribed deformations, was applied. For each load step an incremental, iterative method was used to find a solution.

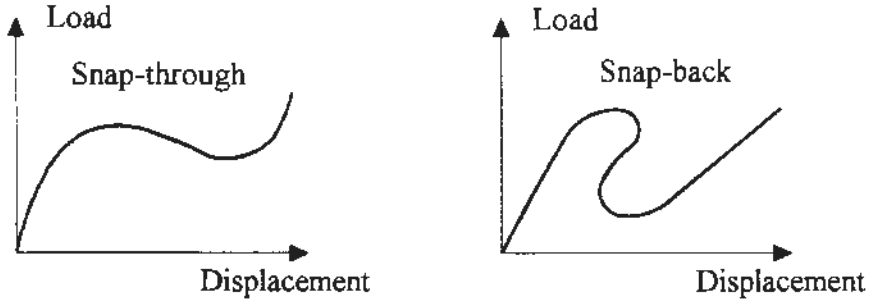

Fig. 11. Snap-through and snap-back behaviour in load displacement response.

Various iterative solution methods were used in the analyses. The Newton-Raphson method is the standard one in ABAQUS and is normally sufficient if the load increases monotonically. Analyses of reinforced concrete structures often involve, however, local maximum points in load-displacement response with snap-through and snap-back behaviour, see Crisfield /14/, Figure 11. To be able to handle this kind of response, an arc-length method was used. The arc-length method available in ABAQUS is the modified Riks method. However, numerical convergence problems arised often when this method was used. A quasi-Newton method in combination with displacement control was found to be the most useful in some of these cases. In the smeared crack analysis, where the numerical problems with the iterative solution methods became too large, an incremental solution technique with no iterations was tested.

Graphic representation of the different solution methods used, for a one degree of freedom system, is shown in Figure 12. With the quasi-Newton methods the inverted stiffness matrix is updated in an approximate way after each iteration, so that the stiffness matrix remains positive definite, and is completely updated only after a specified number of iterations. With the arc-length method the incremental load is treated as an unknown, and the next point of equilibrium on the equilibrium path is sought at a certain distance from the latest point of equilibrium. The incremental solution technique, with no iterations, was performed by setting the tolerance for the residuals in node forces to a very high value, thus suppressing the iteration process.

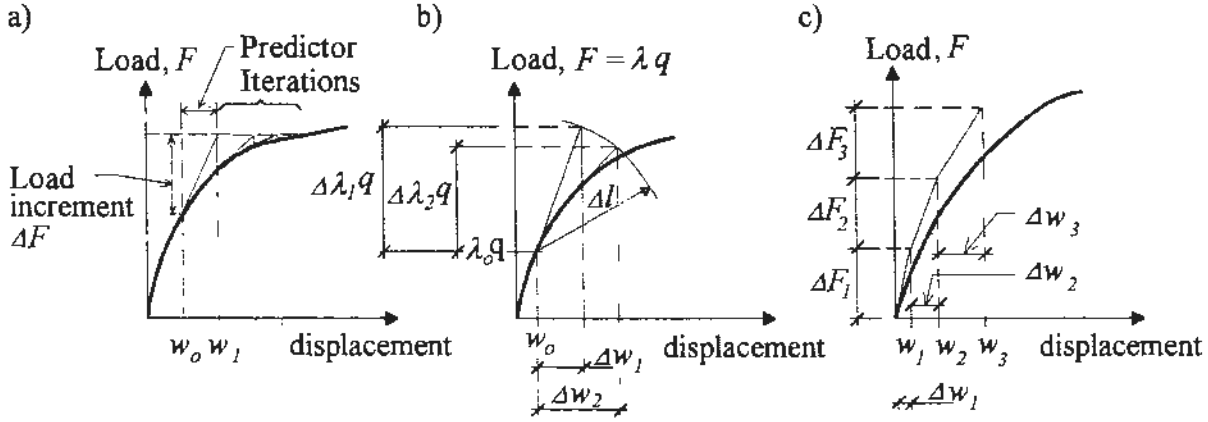

Fig. 12. Solution methods, used in the analyses, for a one degree of freedom system: a) A Newton method (e.g. Regular Newton-Raphson or quasi-Newton), b) Arc-length method, and c) Incremental solution method with no iteration.

4.4 The Load History and Adding of Steel Plates to the Model

Before the bridge was strengthened with glued steel plates, prior to the test, cracks were found at the bottom of the bridge deck. To enable accurate modelling of the response of the bridge during the test, the bridge model was loaded with a "traffic load", corresponding to the traffic load that the bridge was exposed to during its service life time. The traffic load made cracks arise before the steel plate elements were included and the concentrated test load was applied. In the analyses, the traffic load was increased until visible cracks, with a crack width of at least 0.1 mm, were found within the whole area where cracks had been detected before the test. The load history is shown in Figure 13.

In the analysis with the smeared crack approach, where the arc-length method was used, the traffic load was applied as a uniformly distributed load along the bridge deck. In case of the discrete crack approach, where the quasi-Newton method was used in combination with deformation control, the bridge deck was subjected to a prescribed deformation corresponding to the elastic response of a uniformly distributed load. After this model had been subjected to traffic load, the load-displacement relations of the springs were changed as shown in Figure 5, and the rest of the load history was applied in a new analysis. The model with modified properties for the concrete springs was subjected to dead load, before the steel plates were included. For both the smeared and the discrete crack approach, the models were finally subjected to a concentrated load to model the test itself. In the discrete crack analysis, the load was applied through prescribed increasing deformation at the loading point.

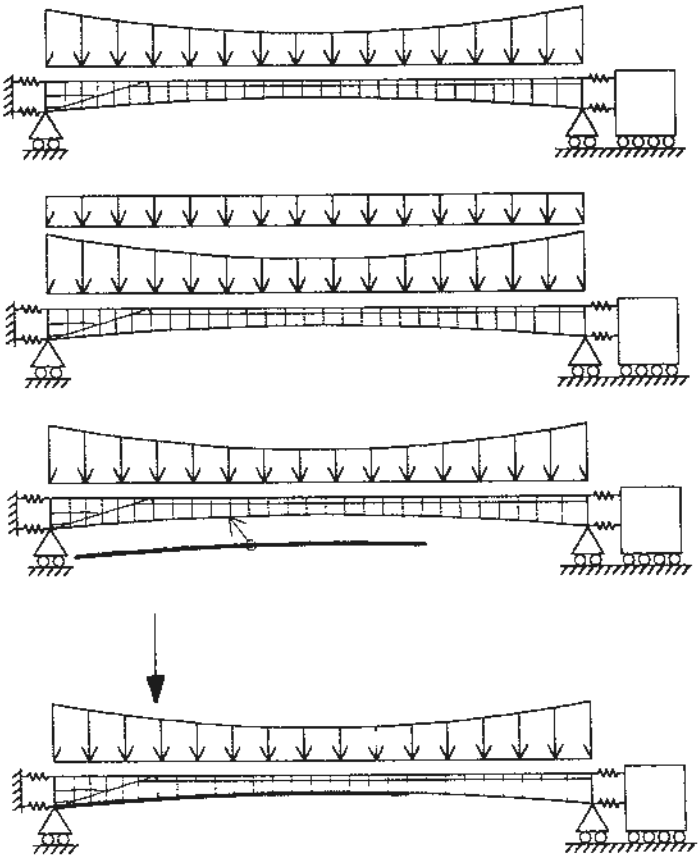

a) The bridge models was first exposed to the dead load of the bridge deck, including pavement

b) The "traffic load" was then added to model the pre-cracking of the bridge

c) After the traffic load was removed, the steel plated was added to the models, while the dead load was still active

d) The bridge models were finally exposed to the concentrated load to model the test itself

Fig. 13. The load history applied to the bridge models in the analyses.

To enable the inclusion of the steel plates in an unstressed condition to the already deformed bridge model, three nodes, *a*, *b* and *c*, were defined at the same positions in the undeformed element mesh, at each connection between the bridge deck elements and the steel plate elements. The nodes *a* were connected to the bridge deck elements, and the nodes *c* to the steel plate elements, while the nodes *b* were not attached to any elements. The deformations, u_i, of the nodes were coupled with the following equation, valid in both degrees of freedom.

$$u_i^{(a)} - u_i^{(b)} - u_i^{(c)} = 0$$

Prescribing the deformations of the nodes *c* to zero, in the first part of the analyses, the free nodes *b* obtained the same deformations as the bridge deck nodes *a*. When the plate elements were made active, the deformations for the free nodes, $u_i^{(b)}$, were fixed to their current values, and the boundary conditions were removed for the steel plate nodes *c*. Further deformations of the bridge gave the steel plate nodes deformations that were equal to the additional deformations of the bridge deck nodes.

4.5 Execution of the Analyses

Several numerical problems were found in the smeared crack analysis. ABAQUS reported both numerical problems with the plasticity algorithm in the material model and convergence problems on structural level. The dead load and the "traffic load" were applied using load control and the standard Newton-Raphson method for iteration. The concentrated load was applied using the modified Riks method. However, the numerical problems became too great when using a reasonably small tolerance, even though the concrete response relation was smoothened in tension. To get a result from the smeared crack analysis, the tolerance was set to a very high value, so that the program should not iterate. Although this method resulted in quite large residuals, even when the load step was divided into the maximum number of increments allowed, it nevertheless gave valuable results regarding the crack distribution.

Convergence problems occurred in the discrete crack analysis as well, but they could be solved by modifying the force-displacement relations for the springs that were connected to the nodes where maximum residuals were found. The response relations were smoothed so that the spring stiffnesses changed more gradually and, in a few springs, by giving the unloading branch in tension a more gradual slope. By this means, these few springs were provided with considerably greater fracture energy, however the influence on the response of the whole structure caused by the increased fracture energy at these few locations was considered to be minor.

Springs where the reinforcement response was superimposed on the concrete response usually achieved a short descending branch in the force-displacement relation when cracking was initiated. To avoid numerical problems, the relations were approximated with a corresponding relation without any dip in the combined response, see Figure 14.

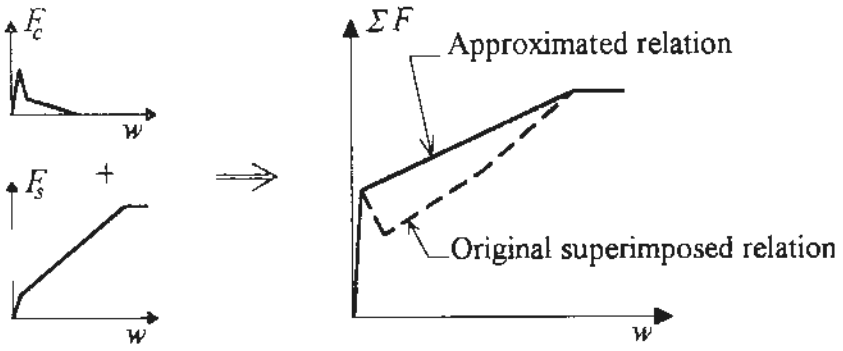

Fig. 14. Example of approximated force-displacement relation for a spring with superimposed reinforcement and concrete response.

4.6 Results of the Analyses

For the smeared crack approach, suppressed iteration in combination with the Riks method gave quite high residuals. Nevertheless, the analysis gave a good picture of the crack pattern in the bridge deck slab, see Figure 15, and it seems that a smeared crack analysis such as this can serve to determine where the necessary crack sections should be pre-defined in a discrete crack analysis. This can be of great value when the structure has not been tested and experience is not sufficient to determine where cracking possibilities should be provided.

The analysis based on the discrete crack approach was performed until the initiation of the shear crack at the load level where failure occurred in the test, see Figure 16. The direction and magnitude of the principal stresses along the pre-defined shear crack were calculated from the result of the analysis, see Figure 17. Biaxial compression was found to occur at both ends of the crack path at crack initiation. The effect of the reinforcement on the shear crack initiation, accordingly, was negligible. The greatest principal tensile stress, 1.75 MPa, occurs at the middle of the shear crack, acting at an angle of about 40° to the longitudinal axis of the bridge.

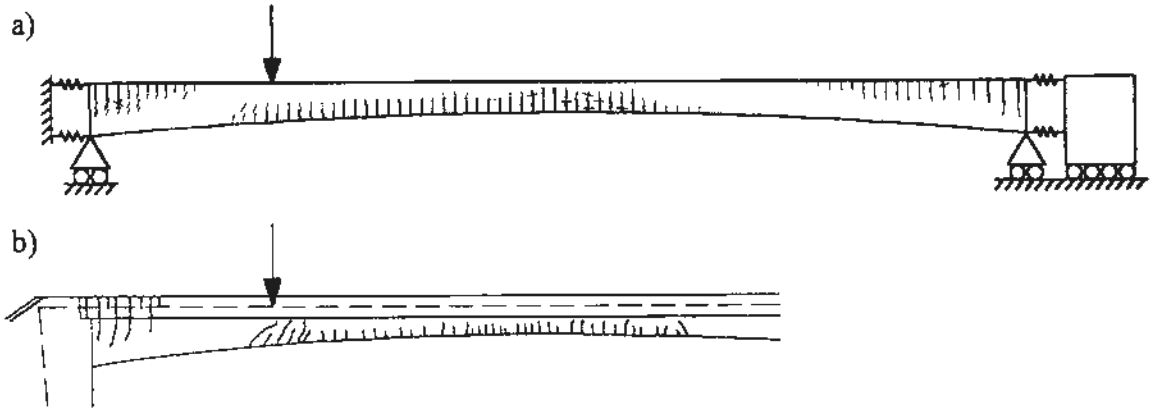

Fig. 15. Crack pattern in the bridge deck slab: a) according to the finite element analysis based on the smeared crack approach. The thicker marks represent visible cracks at maximum load level (crack width, $w \geq 0{,}1$ mm). b) These can be compared with the crack pattern obtained in the test.

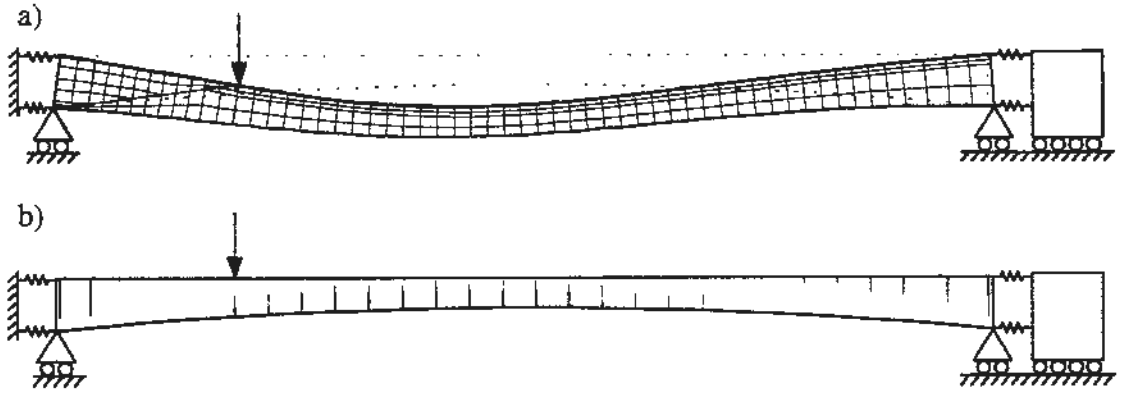

Fig. 16. Results from the discrete crack analysis at maximum load level. Figure a) shows the deformed shape, with the deformations magnified about 13 times, and Figure b) the opened cracks in the model. Cracks visible to the eye ($w \geq 0{,}1$ mm) are marked with thicker lines.

The greatest tensile stress is rather low compared with the tensile strength, as evaluated from splitting tests performed on test cylinders from the bridge. According to the Concrete Handbook Material, see AB Svensk Byggtjänst and Cementa AB /8/, the axial tensile strength is about 80 % of the splitting tensile strength. However, the scatter in the relation between axial and splitting tensile strength is large, as well as in the splitting tests.

The principal tensile stress does not act perpendicular to the pre-defined crack path. A shear crack starts, however, as a zone of microcracks that are perpendicular to the principal tensile stress and connect only later to a major shear crack, see Bazant and Pfeiffer /16/ and Hordijk *et al.* /10/. Thus, the global crack direction does not have to be perpendicular to the principal tensile stress at crack initiation. Since the final crack path had to be pre-defined in the discrete crack model, this behaviour could not be taken into account in a direct manner in the analysis. It should be noted that this behaviour can not be modelled with the smeared crack concrete model in ABAQUS either, since cracks are only allowed to form perpendicular to each other. Even if the initial microcracks are modelled correctly, the final shear crack may not form at the correct angle.

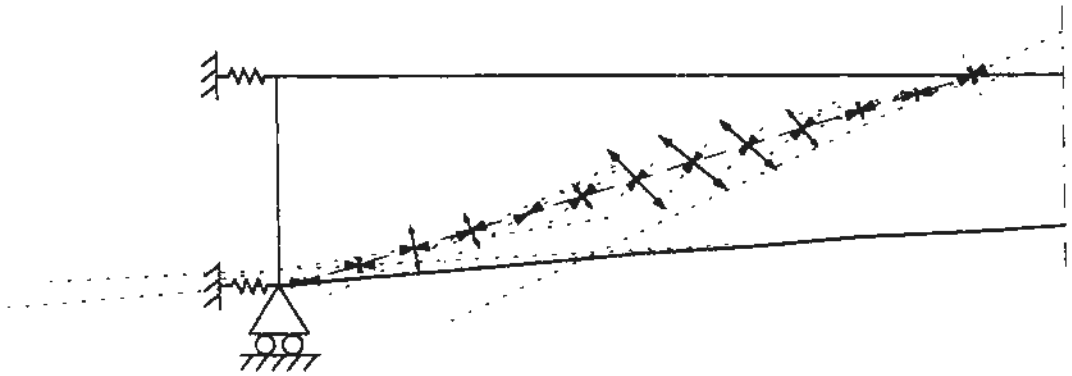

Fig. 17. Principal stresses along the pre-defined shear crack at crack initiation. Thicker arrows are used to show tensile principal stresses (⟵⟶), and dotted arrows are used for compressive principal stresses (⋯⟵⟶⋯).

4.6 Comparison With Test Results

The deflections calculated in the analysis were considerably larger than the deflections measured during the test, see Figure 18. A possible reason for this may be uncertainty regarding the stiffness of the supports. The originally calculated stiffnesses of the support springs were decreased during the first part of the analysis in order to match the crack pattern observed before the test. However, the unrealistic crack pattern, obtained with the original higher stiffnesses, may have been caused by other circumstances. The "traffic load" is indeed unknown and was modelled in a simplified manner, and the concrete strength may have varied between different parts of the bridge.

The tensile strength was reduced in the first part of the analysis in order to obtain a crack development that matched the observations on the tested bridge. The tensile strength was finally approximated to be f_{ct} = 2.5 MPa, which is about 70 % of the splitting tensile strength measured on the cores drilled out of the bridge.

The crack pattern obtained in the analyses agrees well with cracks observed in the test, see Figures 15 and 16. According to the analysis, the shear crack is initiated in the middle of the crack path at an angle that agrees very well with the angle in that position of the shear crack in the test, see Figures 17 and 2. The principal stress direction, measured on the bridge, was nearly the same as in the analysis and the principal stresses were of the same magnitude.

There are probably several reasons why the tensile stress at crack initiation in the analysis was found to be smaller than when it was calculated from the splitting tests. One reason may be the large scatter in the measured splitting strength, and in the relation between splitting strength and

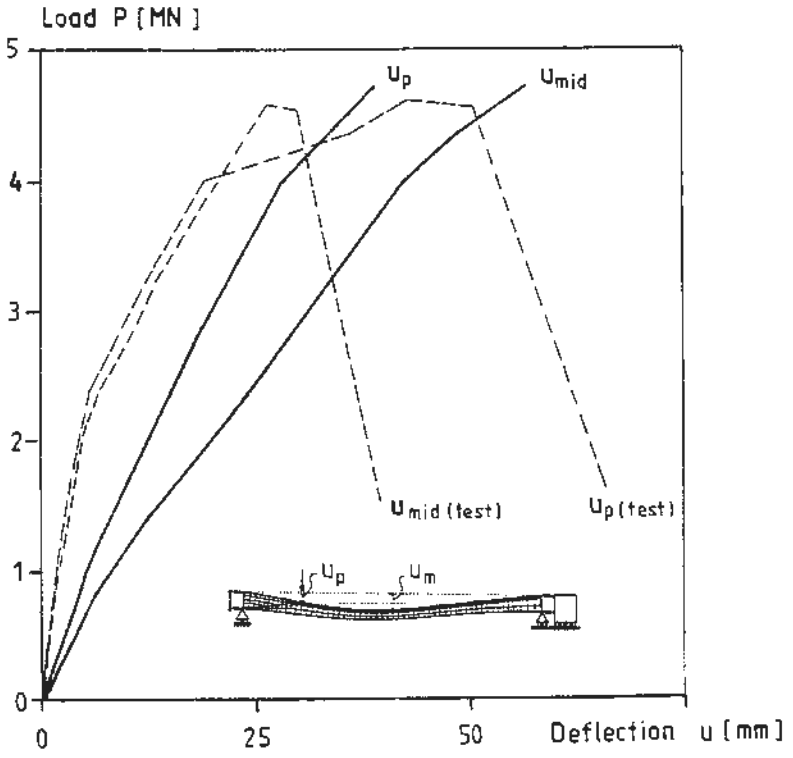

Fig. 18. Load-deflection response obtained in the analysis based on the discrete crack approach. The result of the analysis is compared with the response obtained in the test.

normal tensile strength. Another reason may be that the stiffnesses in the support springs too low, as mentioned above. A greater rigidity of the supports would have given greater longitudinal tensile stresses at the top of the slab close to the support. This would have lead to greater principal tensile stresses in the shear span, as the longitudinal tensile stresses are transferred to the bottom of the slab.

The difference between analysis and test results could also be caused by the fact that the elements in the analysis were quite large in relation to the local phenomena when a crack is initiated. Local peaks in the stress field could not be considered in the analysis. The frame corners were not included in the model, and the vertical reaction forces acted on the model at one node at each support. Since the shear crack ended close to one of the frame corners, this simplified way of modelling the supports may also have affected the accuracy of the analysis.

The results give rise to several suggestions for improvements of the analyses. Instead of reducing the stiffnesses of the supports, the load history of the bridge should be estimated in an alternative manner to achieve the correct pre-cracking. A higher stiffness of the support springs would give a better agreement with the measured load deflection relation. It would also lead to higher principal tensile stresses in the shear span, and a smaller disagreement with the measured tensile strength. Further improvements could be achieved with a higher degree of discretisation, with more elements in the shear zone. Possible local maxima in the stress field would then be easier to detect. If the frame corners had also been included in the model, the distribution of the reaction forces into the structure would be accounted for in a more realistic manner.

5 CONCLUSIONS

The shear failure of the bridge tested was analysed using the finite element method based on non-linear fracture mechanics. Both the smeared and discrete crack approaches were used to model the cracking of concrete. The analyses were performed using the finite element program ABAQUS, HKS /5/.

Numerical problems were found in the non-linear analyses. The analysis based on the smeared crack approach could be carried out only by allowing large residuals. Although this analysis resulted in large errors in the static equilibrium, it gave a good picture of the crack pattern in the bridge deck slab. Consequently, it can be useful in determining where the necessary crack sections shall be pre-defined in a discrete crack analysis. Since the smeared crack approach is more general, it is likely to be used in the future as a powerful tool for detailed analyses, when the numerical problems connected with this method is reduced.

The discrete crack analysis was performed until initiation of the final failure. The analysis shows that the shear crack that led to failure started in the middle of the shear span at about half of the slab height, and had an inclination of about 40° to the longitudinal axis of the bridge. This corresponds very well to the angle of the mid part of the shear crack obtained in the test. The edges of the shear crack path were exposed to biaxial compression at crack initiation.

The maximum principal tensile stress at crack initiation was, in the analysis, quite low compared with the normal tensile strength determined from splitting tensile tests. An explanation for this difference can be found in the large scatter, both in the splitting test results and in the relation

between the splitting tensile strength and the axial tensile strength. Other reasons for the difference may be the uncertainty in the modelling of the rigidity of the supports, and the unknown load history that led to cracking of the bridge during its service life time. The difference that was found between the analysis result and the test result, for the load-deflection relations, is probably also due to these reasons.

It should be noted that neither of the approaches, in the way they were applied here, is absolutely general in the sense that the response of the structure can be completely unknown. When using the discrete crack approach, one has to know the crack pattern in the structure to be able to predefine the crack sections and to specify the correct properties for the crack elements. In the smeared crack approach, used together with the rebar option in ABAQUS, or generally if complete interaction with the surrounding concrete is assumed for the reinforcement, one has to know the mean crack distance in the structure. The reason for this is that the reinforcement in a concrete structure acts as a "crack distributor". The reinforcement acquires a greater force in a section where cracking is initiated. This force is gradually transferred to the surrounding concrete. Consequently, maximum concrete tensile stress cannot occur close to an already initiated crack. In order to model this behaviour correctly, the bond between the reinforcement and the concrete has to be included in the model. If complete interaction is assumed, all concrete elements along a tensioned reinforcement bar will crack, regardless of how small the elements used.

Shear failure is a term that includes several different failure modes and occurs for quite different stress states. Shear failure is actually a whole class of failures and the factors that determine a given failure may vary. To obtain a better understanding of shear failure, it is not sufficient to perform a large amount of different tests, in which the shear force is considered to be the main reason for the failure, and to evaluate the shear capacity from the tests by statistical methods. On the other hand, to analyse the shear tests individually, using the non-linear finite element method in combination with fracture mechanics material models, will lead to a better understanding of the failure process, and the results can serve as a basis for improved design methods.

The use of non-linear fracture mechanics together with the finite element method is believed to be a most powerful tool for describing the mechanical behaviour and obtaining a better understanding of the failure process. Although this method of analysis is still under development, it is already being used in research to improve simplified design methods. In the future it can serve as a tool of analysis used to facilitate improved design of complex structures.

6 ACKNOWLEDGEMENT

The work presented was performed at the Division of Concrete Structures at Chalmers University of Technology, from 1990 to 1992, and was sponsored by the Swedish Council for Building Research.

7 REFERENCES

/1/ Plos, M. (1993): Shear Behaviour in Concrete Bridges - Full Scale Shear Test, Fracture Mechanics Analyses and Evaluation of Code Models. Division of Concrete Structures, Chalmers University of Technology, Publication 93:1, 70 pp.

/2/ Plos, M., Gylltoft, K. and Cederwall, K. (1990): Full-Scale Shear Tests on Modern Highway Concrete Bridges. Nordic Concrete Research, Publication no. 9, The Nordic Concrete Federation, pp. 134-144.

/2/ Plos, M. (1990): Skjuvförsök i full skala på plattrambro i armerad betong (Full-scale shear test on concrete slab frame bridge. In Swedish). Division of concrete structures, Chalmers University of technology, Report 90:3, 117 pp.

/4/ Statens betongkommitté (1988): Bestämmelser för betongkonstruktioner, BBK 79, utgåva 2, Band 1, Konstruktion (Regulations for concrete structures, second edition, Vol. 1, Design. In Swedish). AB Svensk Byggtjänst, 163 pp.

/5/ HKS, Hibbit, Karlsson and Sorensen INC. (1989): ABAQUS, Version 4.8. HKS, Providence, Rhode Island 02906, USA.

/6/ Täljsten B. (1990): Förstärkning av betongkonstruktioner genom pålimmning av stålplåtar (Concrete Structures Strengthened by Externally Bonded Steel Plates, In Swedish). Avdelningen för konstruktionsteknik, Tekniska högskolan i Luleå, licentiatuppsats 1990:06L, 205 pp.

/7/ Elfgren L., editor (1989): Fracture Mechanics of Concrete Structures, From Theory to Applications. Report of the technical committee 90-FMA Fracture Mechanics to Concrete - Application, RILEM. Chapman and Hall, 407 pp.

/8/ AB Svensk Byggtjänst and Cementa AB (1982): Betonghandbok Material (Concrete handbook Material. In Swedish). AB Svensk Byggtjänst, 619 pp.

/9/ Pettersson P-E. (1981): Crack growth and development of fracture zones in plain concrete and similar materials. Division of Building Materials, Lund Institute of Technology, Report TVBM - 1006, 174 pp.

/10/ Hordijk D.A., Van Mier J.G.M. and Reinhardt H.W. (1989): Material Properties. Fracture Mechanics of Concrete Structures, From Theory to Applications (edited by Elfgren), Report of the technical committee 90-FMA Fracture Mechanics to Concrete - Application, RILEM, Chapman and Hall, pp.

/11/ Kupfer H.B. and Gerstle K.H. (1973): Behaviour of Concrete Under Biaxial Stresses. Journal of the Engineering Mechanics Division, ASCE, Vol. 99, pp 853-866.

/12/ Johnsson R.P. and Molenstra I.N. (1991): Partial shear connection in composite beams for buildings. Proceedings of the Institution of Civil Engineers, Part 2, Vol. 91, pp. 679-704.

/13/ Ollgaard J.G., Slutter R.G. and Fisher J.W. (1971): Shear strength of Stud Connectors in Lightweight and Normal-Weight Concrete. AISC Engineering Journal, pp. 55-64.

/14/ CEB, Comite Euro-international du beton (1990): CEB-FIP Model Code 1990, First draft, Chapters 1-5. CEB Bulletin d'information No 195, 217 pp.

/15/ Crisfield M.A. (1986): Snap-Through and Snap-Back Response in Concrete Structures and the Dangers of Under-Integration. International Journal for Numerical Methods in Engineering, Vol. 22, pp. 751-767.

/16/ Bazant Z.P. and Pfeiffer P.A. (1986): Shear fracture tests of concrete. RILEM Materials and Structures, Vol. 19, No. 110, pp. 111-121.

/17/ Plos, M. (1994): Splicing of Reinforcement in Frame Corners: Experimental Studies. Nordic Concrete Research, Publication no. 14. 1/94, The Nordic Concrete Federation, pp. 103-121.